2021

Gene alteration in Zebrafish exposed to a mixture of substances of abuse☆

Bikram Subedi
Murray State University, bsubedi@murraystate.edu

Sydni Anderson
Murray State University

Tara L. Croft
Murray State University, tcroft@murraystate.edu

Eric C. Rouchka
University of Louisville

Mei Zhang
University of Louisville

See next page for additional authors

Recommended Citation

Subedi, B., Anderson, S., Croft, T. L., Rouchka, E. C., Zhang, M., & Hammond-Weinberger, D. R. (2021). Gene alteration in Zebrafish exposed to a mixture of substances of abuse. Environmental Pollution, 116777. https://doi.org/10.1016/j.envpol.2021.116777

Gene alteration in Zebrafish exposed to a mixture of substances of abuse

Subedi, B.[1,*]; Anderson, S.[2]; Croft. T.L.[1]; Rouchka, E.C.[3,4]; Zhang, M.[5], Hammond-Weinberger, D.R.[2]

[1]Department of Chemistry, Murray State University, Murray, Kentucky, United States
[2]Department of Biology, Murray State University, Murray, Kentucky, United States
[3]Department of Computer Science and Engineering, University of Louisville, Louisville, Kentucky, United States
[4]KBRIN Bioinformatics Core, University of Louisville, Louisville, Kentucky, United States
[5]Genomics Facility University of Louisville, Louisville, Kentucky, United States

*Corresponding author: B. Subedi
Department of Chemistry, Murray State University
1201 Jesse D. Jones Hall, Murray, KY 42071
Tel: 1-270-809-6542
Fax: 1-270-809-6474
E-mail: bsubedi@murraystate.edu

KEYWORDS: Illicit Drugs; Psychotic Drugs; Zebrafish; Nervous System; Next Generation Gene Sequencing; RNA-Seq

ABSTRACT

A recent surge in the use and abuse of diverse prescribed psychotic and illicit drugs necessitates the surveillance of drug residues in source water and the associated ecological impacts of chronic exposure to the aquatic organism. Thirty-six psychotic and illicit drug residues were determined in discharged wastewater from two centralized municipal wastewater treatment facilities and two wastewater receiving creeks for seven consecutive days in Kentucky. Zebrafish (*Danio rerio*) larvae were exposed to the environmental relevant mixtures of all drug residues, all illicit drugs, and all prescribed psychotic drugs. The extracted RNA from fish homogenates was sequenced, and differentially expressed sequences were analyzed for known or predicted nervous system

expression, and screened annotated protein-coding genes to the true environmental cocktail mixture. Illicit stimulant (cocaine and one metabolite), opioids (methadone, methadone metabolite, and oxycodone), hallucinogen (MDA), benzodiazepine (oxazepam and temazepam), carbamazepine, and all target selective serotonin reuptake inhibitors including sertraline, fluoxetine, venlafaxine, and citalopram were quantified in 100% of collected samples from both creeks. The high dose cocktail mixture exposure group revealed the largest group of differentially expressed genes: 100 upregulated and 77 downregulated ($p \leq 0.05$; $q \leq 0.05$). The top 20 differentially expressed sequences in each exposure group comprise 82 unique transcripts corresponding to 74% annotated genes, 7% non-coding sequences, and 19% uncharacterized sequences. Among 61 differentially expressed sequences that corresponded to annotated protein-coding genes, 23 (38%) genes or their homologs are known to be expressed in the nervous system of fish or other organisms. Several of the differentially expressed sequences are associated primarily with the immune system, including several major histocompatibility complex class I and interferon-induced proteins. Interleukin-1 beta (downregulated in this study) abnormalities are considered a risk factor for psychosis. This is the first study to assess the contributions of multiple classes of psychotic and illicit drugs in combination with developmental gene expression.

CAPSULE:

Thirty-six psychotic and illicit drug residues determined in surface water and zebrafish exposure to mixtures of those drugs expressed genes that correspond to the CNS and immune system.

1. Introduction

Psychotropic medications are among the most commonly prescribed drugs in the U.S., and 62% of the top 50 prescribed medications target the central nervous system (Fuentes et al., 2018).

Typically, the psychotic, bipolar, schizophrenic, and depressive disorders are treated using a polypharmacy combination of psychotic drugs (Bareis et al., 2018). In addition to a high volume per capita consumption, psychotics and opioids are the most commonly abused classes of the prescribed medications (SAMHSA, 2019). The significant portion of administered benzodiazepines (74.5% of temazepam), selective serotonin reuptake inhibitor (SSRI: 26% of citalopram), opioids (63.8% of codeine), and illicit drugs (36.3% of methamphetamine) is excreted through urine and feces (Baker et al., 2014; Croft et al., 2020).

The consumed (or directly disposed) drugs are discharged down the drain in the form of parent unchanged or metabolites and reach to the wastewater treatment plant (WWTP) or septic systems (Daughton, 1999). The existing wastewater treatment processes and engineering were not designed to remove drug residues; therefore, a significant portion of a mass influx of psychotic and illicit drug residues to the WWTPs end up continuously discharged into the receiving water bodies (Subedi and Kannan, 2014; Subedi and Kannan, 2015). The mass discharge of diverse psychotropic and illicit drugs including methamphetamine (111 mg/d/1000 people), venlafaxine (111 mg/d/1000 people), and EDDP (a metabolite of methadone: 67.5 mg/d/1000 people) were reported from the WWTPs in New York and Kentucky (Subedi and Kannan, 2014; Skees et al., 2018). Continual discharge of drug residues into the source water causes them to behave as pseudo-persistent in the aquatic ecosystem. The amphetamine and methamphetamine were reported as much as 630 ng/L (Lee et al., 2016) and 1994 ng/L (Watanabe et al., 2020) in wastewater impacted Gwynns Falls in Baltimore (MD) and the Foster Creek in Santee (CA), respectively.

Zebrafish (*Danio rerio*) is an important model organism to study complex human neurological disorders due to the physiological and genetic homology to humans, ease of genetic manipulation, robust behavior, and cost-effectiveness (Neelkantan et al., 2013; Bosse and

79 Paterson, 2017). The behavioral alterations on aquatic organisms due to exposure of individual
80 illicit and psychotic drugs, such as cocaine, MDMA, amphetamine, diazepam, are reported. Acute
81 exposure of MDMA at 10-120 mg/L showed significantly altered behaviors of zebrafish adults
82 including bottom swimming, immobility, and impaired intra-session habituation as well as
83 elevated brain *c-fos* expression (Stewart et al., 2011). Exposure of cocaine to the freshwater
84 invertebrate *Daphnia magna* at 50 and 500 ng/L affected the swimming behavior and induced the
85 overproduction of reactive oxygen species (Felice et al., 2019). Similarly, amphetamine-treated
86 artificial streams exhibit several ecological impacts including decreased biofilm chlorophyll *a*
87 (45%) and biofilm gross production (85%) as well as elevated seston (24%) and cumulative
88 dipteran emergence (up to 89%) (Lee et al., 2016). Even though the risk assessment of a mixture
89 of drugs instead of an individual drug in the aquatic environment was suggested (Cerveny et al.,
90 2020), there are very few reports on the ecological effects of exposure to a real-world mixture of
91 diverse classes of psychoactive drugs.

92 The exposure of a mixture of cocaine and its two metabolites (benzoylecgonine and
93 ecgonine methyl) at environmentally relevant levels (~1.0 ug/L) reduced cell viability, increased
94 DNA fragmentation, and altered protein profiles (Parolini et al., 2017; Parolini et al., 2018) in
95 zebrafish embryos and significantly increased lipid peroxidation and DNA damage in the
96 freshwater mussel *Dreissena polymorpha* (Parolini et al., 2013). The exposure of a mixture of
97 acetaminophen, CBZ, gemfibrozil, and venlafaxine to zebrafish for 6 weeks significantly increased
98 the incidence of developmental abnormalities of embryos including spinal cord deformations,
99 pericardial edema, yolk sac edema, and stunted growth (Galus et al., 2013). Zygotic zebrafish
100 exposure to venlafaxine resulted in a higher spatial expression of *nrd4*, a marker of neurogenesis,

and disrupted early brain development as evidence by increased neurogenesis in the hypothalamus, dorsal tuberculum, and preoptic region (Thompson et al., 2017).

The pharmaceutical residues in surface water eventually reach to the drinking water that can cross maternal biological barriers and alter the embryonic nervous system (Kaushik and Thomas, 2019). Mixtures of fluoxetine, venlafaxine, and carbamazepine altered the expression of human neurological genes associated with idiopathic autism, Alzheimer's disease, and schizophrenia in vitro (Kaushik and Thomas, 2019; Kaushik et al., 2016).

In this study, the level of 9 illicit drugs, 20 prescribed psychotic drugs, and 7 select metabolite residues was determined in discharged wastewater effluents and immediately receiving creeks in eastern Kentucky. Zebrafish larvae were exposed to a mixture of all drug residues, all illicit drugs, and all prescribed psychotic drugs at the determined level in creeks. Larvae were also exposed to a mixture of all drugs at the reported highest level elsewhere. The RNA was extracted from fish homogenates for next-generation sequencing, differentially expressed transcripts were analyzed for known or predicted nervous system expression or function, and annotated protein-coding genes screened to the true environmental cocktail mixture. This is the first study to report the developmental gene expression resulting from the exposure to environmental cocktail mixtures of illicit stimulants, hallucinogens, opioids/narcotics as well as prescribed anxiolytics and antidepressants.

2. **Materials and method**

2.1. Reagents and chemicals

The most frequently reported illicit and prescribed antipsychotic drugs in treated wastewater and the receiving water bodies were targeted. The vendor and purity of all reagents

and chemicals including target drugs, metabolites, and corresponding isotope-labeled internal standards are provided elsewhere (Skees et al., 2018).

2.2. Sample collection and preparation

Twenty-four-hour composite samples of treated wastewater (one aliquot every fifteen min) from two WWTPs in eastern Kentucky were collected using a time-proportional autosampler and maintained at 4°C during the collection period. Sampling was performed for seven consecutive days during a typical week in the late summer of 2018. WWTP-A treats an average of 27.2 million gallons per day (MGD) of sewage from industrial and metropolitan areas serving ~190,000 people whereas the WWTP-B treats an average of 21 MGD of sewage from more suburban areas serving ~160,000 people. A creek that receives the treated wastewater effluent discharged from WWTP-A was sampled ~ ½ km downstream while a creek that receives the discharged effluent from WWTP-B was sampled ~1 km downstream. All collected samples were transported on ice to the laboratory and extracted within six hours of collection.

The detailed sample preparation procedures are described elsewhere (Skees et al., 2018; Croft et al., 2020). Briefly, the collected 100 mL of wastewater or 200 mL of surface water samples were allowed to equilibrate to room temperature, thoroughly mixed, centrifuged at 4500 rpm for 5 min, and vacuum filtrated using 1.0 µm glass fiber filter paper to separate suspended particulate matter (SPM). Filtered samples were spiked with internal standards mixture, extracted using Oasis® hydrophilic-lipophilic balance (HLB) solid-phase extraction (SPE) cartridges, and eluted with 4 mL of methanol followed by the 3 mL of 5% ammonia in methanol. The extracts were transferred quantitatively to the amber silanized HPLC vials and the final volume adjusted to 1 mL with methanol. SPM was freeze-dried for 6 h, allowed to reach room temperature, spiked with the internal standard mixture, vortexed with 6 mL of methanol, and ultra-sonicated for 30 min.

SPM samples were then centrifuged, the supernatant liquid was collected, re-extracted and the extracts were combined. All extracts were concentrated to 250 µL under a gentle stream of nitrogen, quantitatively transferred to amber silanized HPLC vials, adjusted the final volume to 1 mL with methanol, and analyzed for target residues using ultra-performance liquid chromatograph (UPLC) tandem mass spectrometer (MS/MS) as detailed elsewhere (Skees et al., 2018; Croft et al., 2020). The isotopic dilution mass spectrometry method was applied where a known quantity of deuterated isotopes of each target analyte (internal standard) is spiked directly into the sample before sample preparation and analytes are quantified based on the relative response factors of isotopic-labeled internal standard and the corresponding analyte. The five-to-ten-point calibration curves of each target analyte were prepared by plotting the concentration-dependent response factor against the response-dependent concentration factor. The linear or quadratic regression coefficients determined using Agilent MassHunter Workstation for the Quantitative Analysis were r^2 ≥0.99 for all analytes. The details of quality assurance and quality control are provided in supporting information.

2.3. Estimation of drug discharge rate

The level of drugs in wastewater and surface water was expressed as the mean (n=7) concentration (ng/L) among seven consecutive days to minimize the potential weekend effect (Table 1). The level of drugs that were detected <LOQ was replaced by LOQ when drugs were quantified in ≥70% of samples. The rate of drug discharge to the receiving creek was determined using equation 1 similar as described elsewhere (Skees et al., 2018).

$$\text{Rate of drug discharge} = C \times F \times \frac{100}{[100 + \text{Stability}]} \times \frac{1}{1\times10^6} \times \frac{1000}{\text{Population}} \quad (1)$$

where *rate of drug discharge* is the daily amount (mg/d/1000 people) of individual drug discharged through wastewater effluent to the creek, *C* is the total nanograms of analytes in 1 L of wastewater

effluent and SPM combined (ng/L), *F* is the daily flow rate of wastewater (L/d) over a 24 h period, *stability* is a measure of stability change (%) of analyte in wastewater up to 12 h (Croft et al., 2020), and the population is the number of people served by WWTPs based on the daily ammoniacal nitrogen load (Croft et al., 2020).

2.4. Animal husbandry

Zebrafish husbandry and experimental procedures were approved by the Murray State Institutional Animal Care and Use Committee. Adult zebrafish (*Danio rerio*) were housed in a recirculating rack system (Aquaneering, San Diego, CA) with a 14:10 light:dark cycle. Water quality was continuously monitored using Neptune APEX (Morgan Hill, CA). The pH ranged between 7.5 and 8 and water temperatures were kept at 27.5 °C ± 1. The zebrafish were fed twice daily with adult zebrafish diet (Ziegler, East Berlin, PA). Eggs were generated by natural spawning. Larvae were raised in 30% Danieau until 72 h post-fertilization (hpf). Hatched zebrafish larvae were maintained at 28.5°C in static tanks of 0.5 L 30% Danieau (17.4 mM NaCl, 0.21 mM KCl, 0.12 mM $MgSO_4$, 0.18 mM $Ca(NO_3)_2$, 1.5 mM HEPES buffer; pH 7.6) with 100% water changes every two days for 14 days. Larvae were fed twice daily with the Golden Pearl powdered larval diet.

2.5. Drug exposure to Zebrafish

Groups of 45 larvae per tank from mixed clutches were exposed to one of three separate sets of drug mixtures [prescribed psychotic drugs (PPD), illicit drugs (ILD), and the cocktail of all prescribed and illicit drugs (PID) at the average concentrations measured in creek A and B. The drug mixtures at the average concentrations measured in creek A and B (Table 1) are represented hereafter as low dose (LD) cocktail mixtures. As a representation of worst-case environmental exposure of neuropsychiatric and illicit drugs, another set of larvae was exposed to a cocktail

192 mixture of all target drugs at the highest concentrations reported in wastewater, represented
193 hereafter as high dose (HD) cocktail mixture (Table S1). An additional set of larvae was considered
194 a vehicle control. The drug mixtures contained acetonitrile and methanol as a vehicle. The amount
195 of each to be added to the exposure tanks was calculated based on the drug mixtures, such that all
196 tanks received the same concentrations of methanol and acetonitrile, regardless of drug mixture.
197 The control groups were dosed with 10 µL acetonitrile and 140 µL methanol in 500 mL 30%
198 Danieau for a final concentration of 20 pL/mL acetonitrile and 280 pL/mL methanol. The
199 experiment was repeated four times with staggered start dates. Larvae were counted during water
200 changes and deceased larvae were removed. Survival analyses were conducted using GraphPad
201 Prism 7.

202 *2.6. RNA extraction and gene expression analysis*

203 After 14 days of drug exposure, larvae were pooled from each tank for total RNA extraction
204 using TRIzol™ reagent according to the manufacturer's recommendations. Larvae were
205 anesthetized on ice and homogenized in TRIzol™ using sterile pestles and by drawing up and
206 down through a 28 G x ½" syringe needle. Homogenized samples were purified using chloroform,
207 precipitated for 10 min at room temperature with glycogen (0.04 µg/µL) and isopropanol, rinsed
208 with chilled 75% ethanol, resuspended in nuclease-free water, and stored at -80°C. Sample
209 concentrations and purity were measured on a NanoDrop Lite Spectrophotometer (ThermoFisher).

210 Libraries were prepared using the TruSeq Stranded mRNA Library Prep kit (Illumina),
211 TruSeq RNA Single Indexes Set A (Illumina), and Set B (Illumina). Poly-A enrichment and RNA
212 fragmentation were performed by treating 100 ng of samples with RNA purification beads,
213 denatured for 5 min at 65°C, washed, and captured polyadenylated RNA at 80°C for 2 min. The
214 mRNA is further purified in a second bead clean-up, fragmented and primed during elution, and

incubating for 8 min at 94°C. After fragmentation, 17 µL of supernatant was removed from the beads and proceeded immediately to synthesize the first-strand cDNA. First Strand cDNA was synthesized mixing 8 µL of First-Strand Synthesis Mix Act D and SuperScript II mix to each sample and heated on a thermocycler. The second strand cDNA was synthesized using Second Strand Marking Mix, incubated at 16°C for 1 h, purified using Agencourt AMPure XP Beads, and eluted using resuspension buffer. A-Tailing Mix was added to the purified samples for Adenylate 3' Ends. Samples were ligated using Ligation Mix, incubated for 30°C for 10 min, purified two times using Agencourt AMPure XP Beads, and 20 µL of the elute was collected for DNA enrichment. DNA fragments were enriched using PCR Primer Cocktail Mix and PCR Master Mix, purified using Agencourt AMPure XP Beads, and 20 µL of eluted libraries were collected and stored at -20°C. The libraries were quantitated using Qubit dsDNA HS Assay Kit (Invitrogen Q32851), diluted, and normalized to the optimal range for Agilent Bioanalyzer analysis using the DNA High Sensitivity Kit (Agilent Technologies). The same molar amounts of libraries were pooled based on the molar concentration from Bioanalyzer. The qualitative and quantitative analyses of pooled libraries were performed on MiSeq using MiSeq Reagent Nano Kit V2 300 cycles (Illumina). Library and PhIX control (Illumina) were denatured and diluted using the manufacturer's standard normalization procedure to the final concentration of 6 pM. An aliquot of the library (300 µL) and PhIX (300 µL) were combined and sequenced on Illumina MiSeq. Based on MiSeq results, an equal amount of libraries was re-pooled prior to the replicate (n=2) NextSeq analysis using Illumina NextSeq 500 (NextSeq 500/550 75 cycle High Output Kit v2) at the University of Louisville Genomics Facility.

The quality of each raw sequence data using FastQC (version 0.10.1) demonstrated the quality of data and no sequence trimming was required. Therefore, the concentrated sequences

were directly aligned to the *Danio rerio* (Zebrafish) reference genome assembly (GRCz11.fa) using STAR (version 2.6) (Dobin et al., 2013), the alignment rate ranged from 96.5 to 98.0%. The differential expression was performed using DESeq2 (Love et al., 2014) and Cuffdiff2 (Trapnell et al., 2012).

Differentially expressed genes at $p \leq 0.05$; $q \leq 0.01$ and $|\log2FC| \geq 0$ were used for further analysis of enriched Gene Ontology Biological Processes (GO:BP) and KEGG Pathways using categoryCompare. The Entrez gene ID for each differentially expressed gene was obtained from the zebrafish Entrez IDs database from NCBI.

The top twenty differentially expressed sequences in each exposure condition were analyzed for known or predicted nervous system expression or function. First, zebrafish sequences that did not have descriptive gene name (ex. si:ch211-157j23.2) were compared to related sequences by translated nucleotide to protein BLAST (blastx) on both NCBI (Johnson et al., 2008) and Ensembl Genome Browser GRCz11 databases (Yates et al., 2020). Sequences were sorted into annotated protein-coding genes, non-coding sequences, and uncharacterized transcripts.

Next, annotated protein-coding genes identified were screened for nervous system expression and/or function. Gene identities were searched on GeneCards.org, with expression analysis containing expression information compiled from RNAseq, microarray, SAGE, and protein expression of human genes (Stelzer et al., 2016). Expression at or above the 10 thresholds in two or more of the datasets (RNAseq, microarray, or SAGE) or ≥ 1 ppm protein was considered "verified" nervous system expression. Literature searches for nervous system expression or function supplemented the expression datasets. ZFIN.org gene expression databases (RNAseq, microarray, in situ hybridization) were also searched for zebrafish nervous system expression.

Several sequences were identified with low resolution – ex. expression in the embryonic head region. Such sequences were classified as nervous system expression "predicted."

3. Results and discussion

3.1. Rate of drug discharge from WWTPs

The majority of the target drugs were discharged to the creek at a weekly average level of 4.67 ng/L (hydromorphone) to 858 ng/L (Heroin) from WWTP-A and 2.79 ng/L (diazepam) to 402 ng/L (Heroin) from WWTP-B through the treated wastewater (Table S1). Two stimulants (methamphetamine and methylphenidate), two opioids (methadone/EDDP and oxycodone), one hallucinogen (MDA), four sedatives (alprazolam, oxazepam, temazepam, and carbamazepine), and all four major antidepressants (venlafaxine, sertraline, fluoxetine, and citalopram) were found in all wastewater samples (detection frequency, df=100%) in both WWTPs.

Our previous study reported 387 g daily mass load of cocaine (sum of cocaine and its two major metabolites in wastewater influent) to WWTP-A and 1030 g to WWTP-B (Croft et al., 2020). In this study, the total daily discharge mass of cocaine from WWTP-A and WWTP-B was 7.15 g and 6.64 g, respectively (Table 1). Based on the level of drug residues quantified in simultaneously collected wastewater influents (Croft et al., 2020) and effluents (this study), the removal efficiencies of cocaine were 98 and 99%, respectively, in WWTP-A and WWTP-B.

The estimated levels of community prevalence of methamphetamine and amphetamine in western Kentucky were highest among the global communities (SCORE, 2019), however, the methamphetamine prevalence in two urban communities in Eastern Kentucky was significantly lower than in rural western Kentucky (Croft et al., 2020). Nonetheless, the average daily mass discharge of methamphetamine and amphetamine from the target WWTPs was ~2500 g and ~675 g, respectively (Table 1). Heroin was predominantly discharged from both WWTPs among opioids

283 followed by methadone, oxycodone, and hydrocodone. Alprazolam is the third most prescribed
284 controlled substance only after hydrocodone and oxycodone in Kentucky (KIPRC, 2019;
285 KASPER, 2020). However, alprazolam was significantly removed (~77%) during the wastewater
286 treatment and lowers the mass discharge of alprazolam from WWTPs compared to temazepam by
287 ~10 folds even though their mass loads to the WWTPs were similar (Croft et al., 2020).
288 Carbamazepine was very stringent on removal through wastewater treatment (Subedi and Kannan,
289 2015) and discharged at ~16.5 g/d in this study. Venlafaxine, sertraline, fluoxetine, and citalopram
290 are among the top 50 most prescribed drugs in the U.S., and the latter three are the top three
291 prescribed selective serotonin reuptake inhibitors (SSRI) in the U.S. (Fuentes et al., 2018).
292 Antidepressants were found to discharge from WWTPs at ~4.0 g/d (fluoxetine) to ~42.0 g/d
293 (venlafaxine) (Table 1).

294 *3.2. Drugs in treated wastewater receiving creeks*

295 The level of drugs in immediate creeks that receive treated wastewater from WWTPs
296 ranged from 2.02 ng/L (cocaethylene, a metabolite of cocaine) to 434 ng/L (Heroin) (Figure 1,
297 Table 1). Overall, a creek that runs through the urban area and receives treated wastewater from a
298 WWTP that treats wastewater from urban areas (WWTP-A) had higher levels of residual drugs.
299 Cocaine (and its one metabolite), methadone (and its metabolite), oxycodone, MDA, oxazepam,
300 temazepam, carbamazepine, and all antidepressants (sertraline, fluoxetine, venlafaxine, and
301 citalopram) were quantified in all samples from both creeks.

302 The ratio of cocaine and its primary metabolite, benzoylecgonine, is typically within a
303 range of 0.27-0.75 based on their human excretion rates and the molar masses (Bijlsma et al.,
304 2012). In this study, the ratio of cocaine and benzoylecgonine (cocaine metabolite) concentrations
305 in creek B (1.55 and 2.18) was higher than in creek A (0.50-0.90), wastewater influents (0.32-

306 0.55), and wastewater effluents (0.28-0.61), suggesting the direct disposal of cocaine in creek B.
307 The use of methamphetamine was significantly higher in rural communities in western Kentucky
308 than urban communities in eastern Kentucky (Croft et al., 2020), and the level of
309 methamphetamine in creek-A (this study) was ~5 folds lower than that reported in Bee Creek in
310 western Kentucky (Skees et al., 2018).

311 There are growing concerns over the upsurge opioid discharges into the source water
312 resulted from the recent elevated opioid consumption in the U.S. Morphine (83 ng/L Lee et al.,
313 2016 in Gwynns Run in Baltimore, Maryland, hydrocodone (126 ng/L Skees et al., 2018) in Bee
314 Creek in western Kentucky, and 71.7 ng/L of EDDP (a metabolite of methadone, this study)
315 suggest the prevalence of opioids in treated wastewater receiving water bodies in the U.S.

316 Very few reports are available on the occurrence of illicit and prescribed antipsychotic
317 drugs of potential abuse and addiction in surface water in the U.S. The majority of drug residues
318 are reported <50 ng/L; however, carbamazepine and select antidepressants such as venlafaxine and
319 citalopram are typically reported ~100 ng/L owing partially to higher production and consumption
320 as well as stringency on removal through conventional wastewater treatment. Despite low ng/L to
321 low µg/L level of drug residues in an aquatic ecosystem, chronic exposure of the aquatic organism
322 to the cocktail environmental mixture of illicit and antipsychotic drug residues can lead to additive
323 or non-additive effects or neutralize each other's effects (Brodin et al., 2014).

324 *3.3. Differentially expressed genes*

325 Larval survival between exposure groups and between exposure replicates was similar.
326 Average 14 dpf survival was 58% (Figure S1) and survival between groups was similar ($F(4, 15) = 1.546$; $p > 0.05$). A Principal Component Analysis performed on the gene sequences obtained
328 from the zebrafish exposure conditions did not find a clear separation between the five

329 experimental groups (Figure S2). Adverse effects on gene expression would likely be even more
330 pronounced and with more variation, if fish were exposed as newly fertilized eggs, as the chorions
331 limit the movement of some compounds (Pelka et al., 2017). However, dechorionation prior to
332 natural hatching does not accurately represent developmental exposure, hence our use of hatched
333 larvae.

334 We detected differentially expressed sequences in developing zebrafish following two
335 weeks of exposure following hatching. When compared to the control condition, the high dose
336 cocktail exposure group revealed the largest group of differentially expressed genes: 100
337 upregulated, 77 downregulated ($p \leq 0.05$; $q \leq 0.05$). The top enriched GO:BP terms were
338 associated with immune responses, cell cycle, and circadian rhythms.

339 Differentially expressed genes fell into one of three categories: named protein-coding
340 genes, non-coding RNAs and pseudogenes, and uncharacterized transcripts. BLAST analyses were
341 used to identify homologous sequences from other species to identify unannotated zebrafish
342 protein-coding genes. The top 20 differentially expressed sequences in each exposure group
343 compared to control represented 82 unique transcripts. These corresponded to 74% annotated
344 genes (**Table S2**), 7% non-coding sequences (**Table S3**), and 19% uncharacterized sequences
345 (**Table S4**). Among 61 differentially expressed sequences that corresponded to annotated protein-
346 coding genes, 10 (16 %) genes or their homologs are known to be functional in the nervous system
347 of fish or other organisms (**Table S2**) and 28 (46%) are predicted to function in the nervous system
348 based on reported gene expression. The remaining 23 genes (38%) have insufficient functional or
349 expression data to verify or predict their functions in the nervous sytem.

350 Of those genes that were previously identified in the nervous system, only a handful have
351 identified nervous system functions – sacsin, plekstrin, mcm7, retreg1, nr1d1, and p2rx7. Sacsin

352 is a molecular chaperone protein (Anderson et al., 2011) that has been linked to cerebellar ataxia
353 in mice (Lariviere et al., 2019; Lariviere et al., 2015; Takiyama, 2007) and was upregulated
354 following high dose drug exposure. Upregulation following drug exposure may indicate increased
355 need for chaperone proteins due to cellular stress. Pleckstrin is a major protein kinase C substrate
356 found in platelets that was upregulated following prescribed drug exposure. Pleckstrin has only
357 recently been described in the nervous system, where it is associated with the cytoskeleton of
358 growing neurites in cultured cells (Guo et al., 2019) and the spiral ganglion neurons in the adult
359 mouse cochlea (Lezirovitz et al., 2020). In situ hybridization reveals widespread, unspecified
360 expression in the zebrafish head (Thisse and Thisse, 2004), suggesting pleckstrin may also be
361 involved in zebrafish neurite growth, though the effect pleckstrin upregulation following drug
362 exposure is unclear. Mcm7 is a minichromosome maintenance complex protein that is involved in
363 the G1 to S phase transition of the cell cycle, and is expressed in CNS neurons and glia following
364 injury (Chen et al. 2013). Mcm7 is also expressed in Down syndrome models of neuroblast
365 proliferation (Hewitt et al., 2010). While the expression and function of mcm7 in zebrafish are
366 unknown, we expect mcm7 is associated with areas of proliferation and its upregulation following
367 drug exposure may be in response to neuronal insult. Retreg1 encodes an ER-Golgi processing
368 protein involved in negative regulation of apoptosis and reticulophagy (Khaminets et al., 2015).
369 Retreg1 is necessary for the survival of nociceptive and autonomic ganglion neurons (Kurth et al.,
370 2009), though its function in zebrafish is untested. The drug exposure-induced downregulation of
371 retreg1 suggests more cells are at risk of apoptosis. Nr1d1 is expressed in the superchiasmatic
372 nucleus of the hypothalamus, retina, pineal gland, and superior colliculus, where it is involved in
373 circadian rhythms (Ueda et al., 2005), though the effects of nr1d1 downregulation following drug
374 exposure are unclear. P2rx7 is a purinergic receptor involved in calcium transport in several

neuronal cell types in other species (Metzger et al., 2017) including hippocampal neurons (Sperlágh et al., 2002), and in several regions of the zebrafish CNS (Appelbaum et al., 2007). P2rx7 is also responsible for the ATP-dependent lysis of macrophages (Lammas et al., 1997). P2rx7 downregulation could be associated with increased immune activity or changes in calcium transport in stressed cells.

Several annotated genes (mov10b.2, mmp9, slc47a2.2, cmpk2, igfbp1b, hamp, hspb9, dusp27, aste1a, vgll1, and mfap4) are expressed in the nervous system of zebrafish or other species but the functions therein are currently speculative (**Table S2**). MOV10, the human homolog of mov10b.2, is an RNA helicase involved in microRNA-mediated gene silencing (Meister et al., 2005). MOV10 is expressed in a wide variety of tissues, including the nervous system (Skariah et al., 2017). The zebrafish mov10b.2 gene may be involved in microRNA related regulation of gene expression in the developing nervous system and its upregulation could have wide-ranging effects on transcription. Mmp9 encodes a matrix metallopeptidase that is best characterized for its roles in normal physiological breakdown of extracellular matrix and immune responses, though it is also expressed in the regenerating zebrafish retina (Kaur et al., 2018; Sharma et al., 2019), where it may be involved in remodeling the extracellular matrix to allow axonal regeneration. Downregulation of mmp9 may be associated with the slowing of normal cellular processes during stress, which could affect axon outgrowth and pathfinding. Slc47a2.2 is uncharacterized in zebrafish, though the widely expressed mammalian homolog is linked to excretion of toxins (Otsuka et al., 2005) which is unsurprising, given that the conditions of the present study resulted in slc47a2.2 upregulation. Cmpk2 is a nucleoside monophosate kinase in mitochondria that is present in all zebrafish tissues, including the nervous system, that is upregulated in response to immune activation (Liu et al., 2019). Igfbp1b encodes an insulin-like growth factor binding protein

398 that is enriched in the liver of zebrafish (Kamei et al., 2008), as is its mammalian homolog, and
399 the drug exposure-induced differential gene expression is most likely due to changes in liver
400 expression. However, igfbp1 is expressed in the fetal brains of rhesus monkeys (Lee et al., 2001),
401 where it functions in growth factor signaling. Similarly, the differential expression in the current
402 study of hamp, hepcidin antimicrobial peptide and iron regulatory hormone, is likely due to
403 changes in liver expression, where hamp is produced during conditions of inflammation (Nemeth
404 et al., 2004a) or high iron (Nemeth et al., 2004b). Why drug exposure led to hamp downregulation
405 is unclear. Hamp is expressed in neural tissues (Zechel et al. 2006), including the hippocampus
406 where plays a role in social recognition (Ji et al., 2019), though exact mechanisms are not yet clear.
407 Hspb9 (heat shock protein family B (small) 9) is also abundant in the d liver (Stelzer et al., 2016),
408 which could represent the differential expression caused by drug exposure. However, hspb9 is also
409 expressed in the hindbrain (Marvin et al., 2008), though the function therein and the effects of
410 hspb9 downregulation are unclear. Dusp27 (alias STYXL2 – serine/threonine/tyrosine interacting
411 like 2) is a phosphatase that is expressed in the zebrafish optic tectum and somites, where it is
412 required for assembly of the muscle contraction apparatus (Fero et al., 2014). Requirements for
413 dusp27 in the nervous system are not yet understood and the drug-associated downregulation may
414 be associated with changes in muscle expression. Aste1a is a homolog of the drosophila asteroid
415 whose function in zebrafish is as yet unknown. ASTE1, the human homolog of aste1a, is expressed
416 neural tissues (Uhlén et al., 2015), though the functions in neural tissues are uncharacterized.
417 VGLL1 is a poorly characterized transcription factor that is expressed in the neural ectoderm
418 (Fasano et al., 2010), though its function therein is unknown. Mfap4 exists in multiple copies in
419 zebrafish and is expressed in primarily macrophages, including brain macrophages (a population
420 distinct from microglia) that are present in the perivascular spaces (Wu et al., 2018) where it is

421 involved in cellular adhesion. Mammals also express MFAP4 in the hypothalamus (Ferran et al.,
422 2015). Therefore, Mfap4 downregulation is most likely associated with immune responses rather
423 than nervous system development.

424 Furthermore, an additional 34 (56%) of the annotated differentially expressed sequences
425 (sepina7, dhx58, fbxo32, rsad2, ftr86, col14a1b, and calcoco1) (**Table S2**) or their homologs are
426 predicted to be expressed in the nervous system, based on previously published low-resolution
427 expression in the head via large scale in situ hybridization, RNA sequencing, or proteomics, which
428 leaves potential nervous system functions even more speculative. Some of these genes are
429 confirmed or predicted to be expressed in the nervous system, though differential expression
430 observed in the current study is likely to do other tissues, particularly as some of these genes are
431 ubiquitously expressed, or nearly so. Serpina7 is a thyroxine-binding globulin expressed in the
432 blood and liver (Kiba et al., 2009) that was downregulated in each condition that featured
433 prescribed drugs. The differential expression of serpina7 in the present study may indeed be due
434 to changes in liver expression. However, serpina7 may also be expressed in the nervous system,
435 as in situ hybridization reveals widespread, unspecified expression in the developing zebrafish
436 head (Thisse and Thisse, 2004) and proteomics estimate mild enrichment of serpina7 in the
437 cerebral cortex (Stelzer et al., 2016), though its potential function in neural tissue is unclear. Dhx58
438 is a predicted component of innate immune signaling in mammals, where it is also expressed in
439 the nervous system (Uhlén et al., 2015). Whether the zebrafish dhx58 is expressed or functions in
440 the CNS is unknown and the differential gene expression following drug exposure may be due to
441 changes in immune tissues. The gene product of fbxo32 contains an F-box, which is associated
442 with phosphorylation-dependent ubiquitination (Bodine et al., 2001). The human FBXO32 is
443 necessary for autophagosome formation and overexpression in neurons can trigger apoptosis

444 (Murdoch et al., 2016). The zebrafish fbxo32 is expressed in several tissues, though is enriched in
445 muscle tissue (Bühler et al., 2016). Fbxo32 downregulation following drug exposure may protect
446 vulnerable cells from apoptosis. Rsad2 is an interferon-induced antiviral protein that is expressed
447 in several tissues, including the brain (Uhlén et al., 2015). The upregulation of rsad2 following
448 drug exposure is most likely due to changes in other body tissues with higher rsad2 expression.
449 Ftr86 is homologous to human TRIM29, a minimally characterized DNA-binding protein is linked
450 to immune system regulation, with unresolved nervous system expression in humans (Uhlén et al.,
451 2015; Stelzer et al., 2016). It is not known to be expressed in the nervous system and the differential
452 expression of ftr86 is likely due to immune system activation. Col14a1b was upregulated following
453 high dose drug exposure. Collagens are not expressed in the central nervous system (except in the
454 meninges), though they are associated with the peripheral nervous system. This differentially
455 expressed collagen is associated with cartilage (Bader et al., 2013) and may represent changes in
456 neural crest gene expression. The transcription factor calcoco1b is poorly characterized in
457 zebrafish, though its human orthologue CALCOCO1 is a nuclear receptor coactivator expressed
458 in many tissues and enriched in the nervous system (Uhlén et al., 2015). Functional data for many
459 of these genes is lacking, making it difficult to predict their potential roles in nervous system
460 development or function. In these cases, the low resolution gene expression data is thus far the
461 best indication that these genes are indeed somehow influencing nervous system development.
462 Several of the differentially expressed sequences are poorly characterized in zebrafish and
463 similar genes were identified through BLAST alignments. As such, it is tenuous to make
464 predictions about the functions of these genes. The largest group of annotated genes are very poorly
465 characterized and have limited expression data. These genes (Cystatin-like protein, NLRC3-like,
466 FAM111a-like, probable E3 ubiquitin-protein ligase HERC4-like, tetraspanin-like, nxpe family

member 3-like, retinol dehydrogenase 12-like, pleckstrin homology domain-containing family member S 1-like, ER-Golgi intermediate compartment protein 2-like, pgbd4-like, GTPase IMAP family member 7-like, NACHT LRR and PDYD domains-containing protein 12 and 3-like, tubb4bl, interferon-induced very large GTPase 1-like, CLEC4M, jac9, and klhl38b), are neither described as expressed in the nervous system or absent from the nervous system, leaving it an open question. Klhl38b represents a gene duplication in zebrafish of a poorly characterized transcriptional enhancer. The mammalian KLHL38 homolog is primarily expressed in muscle (Ehrlich et al., 2020), though nervous system expression remains possible. As such, the differential expression in the present study of klhl38b most likely represents differential muscle expression. Two remaining genes are sufficiently well-characterized with no described expression in the nervous system that the differential gene expression is likely due to non-neural tissues: mpx is a myeloid-specific peroxidase and hbbe1.1 is an embryonic hemoglobin.

From the differential gene expression of annotated versus novel sequences, plus verified versus predicted nervous system functions, we predict a majority of the differentially regulated genes in this analysis affect nervous system development and/or function. How those changes in gene expression manifest in the organism is beyond the scope of this project. We expect the differential expression of each of these genes to have a minor effect on the organism, and that the summative changes in gene expression may have complex and varied effects on zebrafish. We conclude that exposure to neuroactive compounds induces changes in nervous system gene expression.

3.4. Connections to human disease

Several of the differentially expressed sequences are associated primarily with the immune system, including several major histocompatibility complex class I (MHCI; mhc1lja, mhc1zfa,

mhc1uba, and mhc1lfa) and interferon-induced proteins (ifit44 X1, ifit8, ifit14, and ifit15). Many of the genetic associations linked to schizophrenia in humans converge on immune responses and genes associated with the immune system. In particular, MHCI expression in the brain is altered in schizophrenia (McAllister 2004). Furthermore, cytokine production from immune activation is associated with schizophrenia. Specifically, interleukin-1 beta (downregulated in the present study) abnormalities are considered a risk factor for psychosis (Mostaid et al., 2019) possibly due to its role in guiding the migration of cortical neurons during development (Ma et al., 2014).

Parkinson's disease has complex etiology with both genetic and environmental risk factors and involves abnormal expression of many genes, some of which were detected in this study. Elovl7b is a fatty acid elongase found in most tissues, notably in the oligodendrocytes in the CNS (Keo et al., 2020; Shin et al., 2009) where it functions to extend fatty acids, presumably associated with myelin production. Downregulation of ELOVL7 in oligodendrocytes is associated with Parkinson's susceptibility (Li et al., 2018; Keo et al., 2020). The proteasome activator psme4a promotes ubiquitin-independent protein degradation. Psme4a may be involved in necessary protein recycling in the developing zebrafish. Downregulation of PSME4 has been linked to Parkinson's disease via bioinformatics analysis and confirmed in patients with the disease (Yuan et al., 2020), though causation has not been established.

Other genes that were differentially expressed genes are known to be expressed in brain vasculature, where abnormal gene expression can have neurological consequences. Epgn is an epithelial mitogen homolog that is enriched primarily in epithelial tissues and vasculature, (Stelzer et al. 2016), where its function therein is unexplored. Crp2 and cpr3 encode pentaxin-related proteins that are orthologues to the human CRP gene. Zebrafish crp2 and cpr3 expression patterns are unexplored, though mammalian CRP is expressed in a variety of tissues and is enriched

primarily in epithelial tissues and vasculature, including those within the nervous system, where CRP influences blood-brain-barrier permeability (Hsuchou et al., 2012). Rnf213b is a ring finger protein that possesses both ubiquitin ligase and ATPase activities and is required for normal vascular development in zebrafish (Liu et al., 2011). Whether or not rnf213b is also required in neurons has not been explored, though abnormal vessel sprouting in the developing head could have neurological consequences. Expression of abnormal RNF213 in humans is associated with moyamoya, a rare narrowing of the internal carotid arteries that limits blood to the brain. Due to incomplete penetrance of the disease, RNF213 is postulated to act with environmental factors to result in moyamoya (Koizumi et al., 2015). Our results support the role of the environment in developmental expression of rnf213b.

4. Conclusion

Thirty-six psychotic and illicit drug residues were determined in discharged wastewater from two centralized municipal wastewater treatment facilities and two wastewater receiving creeks in Kentucky. The majority of the target drugs including illicit stimulants as well as potential drug of abuse including opioids, sedatives, and antidepressants were found discharged from the WWTPs to the creek at a weekly average level of 2.79 ng/L (diazepam) to 858 ng/L (Heroin). The weekly level of drugs in immediate receiving creeks ranged from 2.02 ng/L (cocaethylene, a metabolite of cocaine) to 434 ng/L (Heroin). Zebrafish larvae were exposed to the environmental relevant mixtures of all drug residues, all illicit drugs, and all prescribed psychotic drugs. The high dose cocktail mixture exposure revealed the largest group of differentially expressed genes: 100 upregulated and 77 downregulated ($p \leq 0.05$; $q \leq 0.05$). Among 61 differentially expressed sequences that corresponded to annotated protein-coding genes, 23 (38%) genes or their homologs are known to be expressed in the nervous system of

fish or other organisms. Several of the differentially expressed sequences are associated primarily with the immune system, including several major histocompatibility complex class I and interferon-induced proteins. Interleukin-1 beta (downregulated in this study) abnormalities are considered a risk factor for psychosis. To our knowledge, this is the first study to assess the contributions of multiple classes of drugs in combination with developmental gene expression. The fact that these drugs are found in the water bodies that are a potential source of drinking water, humans are also exposed to low-level drugs in combination. This route of exposure is most concerning for pregnant women, as many of these drugs or their metabolites would reach the embryonic brain.

Funding source disclosure

This study was funded by grants from the Kentucky Biomedical Research Infrastructure Network (NIGMS P20GM103436). Sequencing and bioinformatics support for this work provided by National Institutes of Health (NIH) grants P20GM103436 (Nigel Cooper, PI) and P20GM106396 (Donald Miller, PI). The contents of this work are solely the responsibility of the authors and do not represent the official views of the NIH or the National Institute for General Medical Sciences (NIGMS).

Competing interest statement

The authors are not aware of any substantive or perceived competing interest concerning this work.

Acknowledgments

Authors are thankful to The Jones/Ross Research Center at the Department of Chemistry, Murray State University for providing access to the UPLC-MS/MS and Sabnine Waigel, University of Louisville Genomics Facility, for support in the Next Generation Sequencing experiments.

Wastewater treatment plants are acknowledged for providing access to the 24 h composite wastewater samples.

Appendix A. Supplementary data

Supplementary material related to this article can be found, in the online version, at doi xxx

References

Anderson, J. F., Siller, E., Barral, J. M., 2011. The neurodegenerative-disease-related protein sacsin is a molecular chaperone. J. Mol. Biol. 411, 870–880.

Appelbaum, L., Skariah, G., Mourrain, P., Mignot, E., 2007. Comparative expression of p2x receptors and ecto-nucleoside triphosphate diphosphohydrolase 3 in hypocretin and sensory neurons in zebrafish. Brain Res. 1174, 66-75.

Bader, H. L., Lambert, E., Guiraud, A., Malbouyres, M., Driever, W., Koch, M., Ruggiero, F., **2013.** Zebrafish collagen XIV is transiently expressed in epithelia and is required for proper function of certain basement membranes. J. Biol. Chem. 288, 6777–6787.

Baker, D. R.; Barron, L.; Kasprzyk-Hordern, B., 2014. Illicit and pharmaceutical drug consumption estimated via wastewater analysis. Part A: chemical analysis and drug use estimates. Sci. Total Environ. 487, 629–641.

Bareis, N.; Sando, T. A.; Mezuk, B.; Cohen, S. A., 2018. Association between psychotropic medication polypharmacy and an objective measure of balance impairment among middle-aged adults: Results from the US National Health and Nutrition Examination Survey. CNS Drugs 32, 863-871.

Bartelt-Hunt, S. L.; Snow, D. D.; Damon, T.; Shockley, J.; Hoagland, K., 2009. The occurrence of illicit and therapeutic pharmaceuticals in wastewater effluent and surface waters in Nebraska. Environ. Pollut. 157, 786-791.

Bijlsma, L.; Emke, E.; Hernandez, F.; de Voogt, P., 2012. Investigation of drugs of abuse and relevant metabolites in Dutch sewage water by liquid chromatography coupled to high-resolution mass spectrometry. Chemosphere 89, 1399-1406.

Bodine, S. C., Latres, E., Baumhueter, S., Lai, V. K., Nunez, L., Clarke, B. A., Poueymirou, W. T., Panaro, F. J., Na, E., Dharmarajan, K., Pan, Z. Q., Valenzuela, D. M., DeChiara, T. M., Stitt, T. N., Yancopoulos, G. D., Glass, D. J., 2001. Identification of ubiquitin ligases required for skeletal muscle atrophy. Science. 294, 1704-1708.

Bosse, G. D.; Peterson, R. T., 2017. Development of an opioid self-administration assay to study drug seeking in Zebrafish. Behav. Brain Res. 335, 158-166.

Brodin, T.; Piovano, S.; Fick, J.; Klaminder, J.; Heynen, M.; Jonsson, M., 2014. Ecological effects of pharmaceuticals in aquatic systems—impacts through behavioral alterations. Philos. Trans. R. Soc. London, Ser. B. 369, 20130580.

Bühler, A., Kustermann, M., Bummer, T., Rottbauer, W., Sandri, M., Just, S., 2016. Atrogin-1 deficiency leads to myopathy and heart failure in Zebrafish. Int. J. Mol. Sci. 17, 187.

596 Cerveny, D.; Brodin, T.; Cisar, P.; McCallum, E. S.; Fick, J., 2020. Bioconcentration and
597 behavioral effects of four benzodiazepines and their environmentally relevant mixture in
598 wild fish. Sci. Total Environ, 702, 134780.
599 Chen, J., Cui, Z., Li, W., Shen, A., Xu, G., Bao, G., Sun, Y., Wang, L., Fan, J., Zhang, J., Yang,
600 L., Cui, Z., 2013. MCM7 expression is altered in rat after spinal cord injury. J. Mol.
601 Neurosci. 51, 82-91.
602 Croft, T. L., Huffines, R. A., Pathak, M., Subedi, B., 2020. Prevalence of illicit and prescribed
603 neuropsychiatric drugs in three communities in Kentucky using wastewater-based
604 epidemiology and Monte Carlo simulation for the estimation of associated uncertainties. J.
605 Hazard. Mater. 384, 121360.
606 Daughton, C. G.; Ternes, T. A., 1999. Pharmaceuticals and personal care products in the
607 environment: agents of subtle change? Environ. Health Perspect. 107, 907-938.
608 Dobin, A.; Davis, C. A.; Schlesinger, F.; Drenkow, J.; Zaleski, C.; Jha, S.; Batut, P.; Chaisson,
609 M.; Gineras, T. R., 2013. STAR: ultrafast universal RNA-seq aligner. Bioinformatics 29,
610 15-21.
611 Ehrlich, K. C., Baribault, C., Ehrlich, M., 2020. Epigenetics of muscle- and brain-specific
612 expression of KLHL family genes. Int. J. Mol. Sci. 21, 8394.
613 Fasano, C. A., Chambers, S. M., Lee, G., Tomishima, M. J., Studer, L., 2010. Efficient
614 derivation of functional floor plate tissue from human embryonic stem cells. Cell Stem
615 Cell. 6, 336-347.
616 Felice, B. D.; Salguiero-Gonzalez, N.; Castiglioni, S.; Saino, N.; Parolini, M., 2019. Biochemical
617 and behavioral effects induced by cocaine exposure to Daphnia magna. Sci. Total Environ.
618 689, 141-148.
619 Fero, K., Bergeron, S. A., Horstick, E. J., Codore, H., Li, G. H., Ono, F., Dowling, J. J., Burgess,
620 H. A., 2014. Impaired embryonic motility in dusp27 mutants reveals a developmental
621 defect in myofibril structure. Dis. Model Mech. 7, 289-98.
622 Ferran, J. L., Puelles, L., Rubenstein, J. L., 2015. Molecular codes defining rostrocaudal domains
623 in the embryonic mouse hypothalamus. Front Neuroanat. 17, 9-46.
624 Fuentes, A. V; Pineda, M. D.; Venkata, K. C. N., 2018. Comprehension of top 200 prescribed
625 drugs in the US as a resource for pharmacy teaching, training, and practice. Pharmacy 6,
626 43-53.
627 Galus, M.; Jeyaranjann, J.; Smith, E.; Li, H.; Metcalfe, C.; Wilson, J. Y., 2013. Chronic effects
628 of exposure to a pharmaceutical mixture and municipal wastewater in zebrafish. Aquat.
629 Toxicol. 132-133, 212-222.
630 Guo, J., Cai, Y., Ye, X., Ma, N., Wang, Y., Yu, B., Wan, J., 2019. MiR-409-5p as a regulator of
631 neurite growth ss down regulated in APP/PS1 murine model of alzheimer's disease. Front.
632 Neurosci, 13, 1264.
633 Hewitt, C. A., Ling, K. H., Merson, T. D., Simpson, K. M., Ritchie, M. E., King, S. L., Pritchard,
634 M. A., Smyth, G. K., Thomas, T., Scott, H. S., Voss, A. K., 2011. Gene network
635 disruptions and neurogenesis defects in the adult Ts1Cje mouse model of Down
636 syndrome. PLoS One 5, e11561.

637 Hsuchou, H., Kastin, A. J., Mishra, P. K., Pan, W., 2012. C-reactive protein increases BBB
638 permeability: implications for obesity and neuroinflammation. Cell Physiol Biochem. 30,
639 1109-1019.
640 Ji, P., Lönnerdal, B., Kim, K., Jinno, C. N., 2019. Iron over supplementation causes hippocampal
641 iron overloading and impairs social novelty recognition in nursing piglets. J. Nutr. 149,
642 398-405.
643 Johnson, M.; Zaretskaya, I.; Raytselis, Y.; Merezhuk, Y.; McGinnis, S.; Madden, T. L., 2008.
644 NCBI BLAST: a better web interface. Nucleic Acids Res. 36, W5-W9.
645 Kamei, H., Lu, L., Jiao, S., Li, Y., Gyrup, C., Laursen, L. S., Oxvig, C., Zhou, J., Duan, C., 2008.
646 Duplication and diversification of the hypoxia-inducible IGFBP-1 gene in zebrafish.
647 PLoS One 3, e3091.
648 Kaushik, G.; Thomas, M. A., 2019. The potential association of psychoactive pharmaceuticals in
649 the environment with human neurological disorders. Sustainable Chem. Pharm. 13,
650 100148.
651 Kaushik, G., Xia, Y., Yang, L., Thomas, M. A., 2016. Psychoactive pharmaceuticals at
652 environmental concentrations induce in vitro gene expression associated with neurological
653 disorders. BMC Genomics, 17, 435-442.
654 KASPER (Kentucky All Schedule Prescription Electronic Reporting), 2020. Quarterly Trend
655 Report 1st Quarter 2020.
656 https://chfs.ky.gov/agencies/os/oig/dai/deppb/Documents/KASPER_Quarterly_Trend_Re
657 port_Q1_2020.pdf (accessed 2020/11/10).
658 Kaur, S., Gupta, S., Chaudhary, M., Khursheed, M. A., Mitra, S., Kurup, A. J., Ramachandran,
659 R., 2018. let-7 MicroRNA-mediated regulation of Shh signaling and the gene regulatory
660 network is essential for retina regeneration. Cell Rep. 23, 1409-1423.
661 Keo, A., Mahfouz, A., Ingrassia, A. M. T., Meneboo, J. P., Villenet, C., Mutez. E., Comptdaer,
662 T., Lelieveldt. B. P. F., Figeac, M., Chartier-Harlin, M. C., van de Berg, W. D. J., van
663 Hilten. J. J., Reinders, M. J. T., 2020.Transcriptomic signatures of brain regional
664 vulnerability to Parkinson's disease. Commun Biol. 3, 101.
665 Khaminets, A., Heinrich, T., Mari, M., Grumati, P., Huebner, A. K., Akutsu, M., Liebmann, L.,
666 Stolz, A., Nietzsche, S., Koch, N., Mauthe, M., Katona, I., Qualmann, B., Weis, J.,
667 Reggiori, F., Kurth, I., Hübner, C. A., Dikic, I., 2015. Regulation of endoplasmic
668 reticulum turnover by selective autophagy. Nature. 522, 354-358.
669 Kiba, T., Kintaka, Y., Suzuki, Y., Nakata, E., Ishigaki, Y., Inoue, S., 2009. Gene expression
670 profiling in rat liver after VMH lesioning. Exp. Biol. Med. 234, 758–763.
671 KIPRC (Kentucky Injury Prevention and Research Center), 2019. Dose and Overdose report.
672 http://www.mc.uky.edu/kiprc/pubs/overdose/index.html (accessed 2020/11/10)
673 Koizumi, A., Kobayashi, H., Hitomi, T., Harada, K. H., Habu, T., Youssefian, S., 2016. A new
674 horizon of moyamoya disease and associated health risks explored through RNF213.
675 Environ Health Prev Med. 21, 55-70.
676 Kurth, I., Pamminger, T., Hennings, J. C., Soehendra, D., Huebner, A. K., Rotthier, A., Baets, J.,
677 Senderek, J., Topaloglu, H., Farrell, S. A., Nürnberg, G., Nürnberg, P., De Jonghe, P.,
678 Gal, A., Kaether, C., Timmerman, V., Hübner, C. A., 2009. Mutations in FAM134B,

encoding a newly identified Golgi protein, cause severe sensory and autonomic neuropathy. Nat. Genet. 41, 1179-1181.
Lammas, D. A., Stober, C., Harvey, C. J., Kendrick, N., Panchalingam, S., Kumararatne, D. S., 1997. ATP-induced killing of mycobacteria by human macrophages is mediated by purinergic P2Z(P2X7) receptors. Immunity 7, 433-44.
Larivière, R., Gaudet, R., Gentil, B. J., Girard, M., Conte, T. C., Minotti, S., Leclerc-Desaulniers, K., Gehring, K., McKinney, R. A., Shoubridge, E. A., McPherson, P. S., Durham, H. D., Brais, B. 2015. Sacs knockout mice present pathophysiological defects underlying autosomal recessive spastic ataxia of Charlevoix-Saguenay. H. Mol. Genet. 24, 727–739.
Larivière, R., Sgarioto, N., Márquez, B. T., Gaudet, R., Choquet, K., McKinney, R. A., Watt, A. J., Brais, B., 2019. Sacs R272C missense homozygous mice develop an ataxia phenotype. Mol. Brain. 12, 19.
Lee, C. I., Goldstein, O., Han, V. K., Tarantal, A. F., 2001. IGF-II and IGF binding protein (IGFBP-1, IGFBP-3) gene expression in fetal rhesus monkey tissues during the second and third trimesters. Pediatr. Res. 49, 379-387.
Lee, S. S.; Paspalof, A. M.; Snow, D. D.; Richmond, E. K.; Rosi-Marshall, E. J.; Kelly, J. J., 2016. Occurrence and potential biological effects of amphetamine on stream communities. Environ. Sci. Technol. 50, 9727-9735.
Lezirovitz, K., Vieira-Silva, G. A., Batissoco, A. C., Levy, D., Kitajima, J. P., Trouillet, A., Ouyang, E., Zebarjadi, N., Sampaio-Silva, J., Pedroso-Campos, V., Nascimento, L. R., Sonoda, C. Y., Borges, V. M., Vasconcelos, L. G., Beck, R., Grasel, S. S., Jagger, D. J., Grillet, N., Bento, R. F., Mingroni-Netto, R. C., Oiticica, J., 2020. A rare genomic duplication in 2p14 underlies autosomal dominant hearing loss DFNA58. Hum. Mol. Genet. 29, 1520–1536.
Li, G., Cui, S., Du, J., Liu, J., Zhang, P., Fu, Y., He, Y., Zhou, H., Ma, J., Chen, S., 2018. Association of *GALC*, *ZNF184*, *IL1R2* and *ELOVL7* With Parkinson's disease in Southern Chinese. Front Aging Neurosci. 13, 402.
Liu, W., Morito, D., Takashima, S., Mineharu, Y., Kobayashi, H., Hitomi, T., Hashikata, H., Matsuura, N., Yamazaki, S., Toyoda, A., Kikuta, K., Takagi, Y., Harada, K. H., Fujiyama, A., Herzig, R., Krischek, B., Zou, L., Kim, J. E., Kitakaze, M., Miyamoto, S., Nagata, K., Hashimoto, N., Koizumi, A., 2011. Identification of RNF213 as a susceptibility gene for moyamoya disease and its possible role in vascular development. PLoS One 6, e22542.
Liu, W., Chen, B., Chen, Li., Yao, J., Liu, J., Kuang, M., Wang, F., Wang, Y., Elkady, G., Lu, Y., Zhang, Y., Liu, X., 2019. Identification of fish CMPK2 as an interferon stimulated gene against SVCV infection. Fish Shellfish Immunol. 92, 125-132.
Love, M., Anders, S., Huber, W., 2014. Differential analysis of count data-the DESeq2 package. Genome Biol. 15, 550.
Ma, L., Li, X. W., Zhang, S. J., Yang, F., Zhu, G. M., Yuan, X. B., Jiang, W., 2014. Interleukin-1 beta guides the migration of cortical neurons. J. Neuroinflamm. 11, 114.
Marvin, M., O'Rourke, D., Kurihara, T., Juliano, C. E., Harrison, K. L., Hutson, L. D., 2008. Developmental expression patterns of the zebrafish small heat shock proteins. Dev. Dyn. 237, 454-463.

McAllister A. K., 2014. Major histocompatibility complex I in brain development and schizophrenia. Biol. Psychiat. 75, 262–268

Meister, G., Landthaler, M., Peters, L., Chen, P. Y., Urlaub, H., Lührmann, R., Tuschl, T., 2005. Identification of novel argonaute-associated proteins. Curr Biol. 15, 2149-2155.

Metzger, M. W., Walser, S. M., Aprile-Garcia, F., Dedic, N., Chen, A., Holsboer, F., Arzt, E., Wurst, W., Deussing, J. M., 2017. Genetically dissecting P2rx7 expression within the central nervous system using conditional humanized mice. Purinergic Signal. 13, 153-170.

Mostaid, M. S., Dimitrakopoulos, S., Wannan, C., Cropley, V., Weickert, C. S., Everall, I. P., Pantelis, C., Bousman, C. A., 2019. An Interleukin-1 beta (IL1B) haplotype linked with psychosis transition is associated with IL1B gene expression and brain structure. Schizophr. Res. 204, 201–205.

Murdoch, J. D., Rostosky, C. M., Gowrisankaran, S., Arora, A. S., Soukup, S. F., Vidal, R., Capece, V., Freytag, S., Fischer, A., Verstreken, P., Bonn, S., Raimundo, N., Milosevic, I., 2016. Endophilin-A deficiency induces the Foxo3a-Fbxo32 network in the brain and causes dysregulation of autophagy and the ubiquitin-proteasome system. Cell Rep. 17, 1071-1086.

Neelkantan, N.; Mikhaylova, A.; Stewart, A. M.; Arnold, R.; Gjeloshi, V.; Kondaveeti, D.; Poudel, M. K.; Kalueff, A. V., 2013. Perspectives on Zebrafish models of hallucinogenic drugs and related psychotropic compounds. ACS Chem. Neurosci. 4, 1137-1150.

Nemeth, E., Rivera, S., Gabayan, V., Keller, C., Taudorf, S., Pedersen, B. K., Ganz, T., 2004a. IL-6 mediates hypoferremia of inflammation by inducing the synthesis of the iron regulatory hormone hepcidin. J. Clin. Invest. 113, 1271-1276.

Nemeth, E., Tuttle, M. S., Powelson, J., Vaughn, M. B., Donovan, A., Ward, D. M., Ganz, T., Kaplan, J., 2004b. Hepcidin regulates cellular iron efflux by binding to ferroportin and inducing its internalization. Science 306, 2090-2093.

Otsuka, M., Matsumoto, T., Morimoto, R., Arioka, S., Omote, H., Moriyama, Y., 2005. A human transporter protein that mediates the final excretion step for toxic organic cations. Proc. Natl. Acad. Sci. U S A 102, 17923-17928.

Parolini, M.; Bini, L.; Magni, S.; Rizzo, A.; Ghilardi, A.; Landi, C.; Armini, A.; Giacco, L. D.; Binelli, A., 2018. Exposure to cocaine and its main metabolites altered the protein profile of zebrafish embryos. Environ. Pollut. 232, 603-614.

Parolini, M.; Ghilardi, A.; Torre, C. D.; Magni, S.; Prosperi, L.; Calagno, M.; Giacco, L. D.; Binelli, A., 2017. Environmental concentrations of cocaine and its main metabolites modulated antioxidant response and caused cyto-genotoxic effects in zebrafish embryo cells. Environ. Pollut. 226, 504-514.

Parolini, M.; Pedriali, A.; Riva, C.; Binelli, A., 2013. Sub-lethal effects caused by the cocaine metabolite benzoylecgonine to the freshwater mussel *Dreissena polymorpha*. Sci. Total Environ. 444, 43-50.

Pelka, K. E., Henn, K., Keck, A., Sapel, B., Braunbeck, T., 2017. Size does matter - Determination of the critical molecular size for the uptake of chemicals across the chorion of zebrafish (Danio rerio) embryos. Aquat. Toxicol. 185, 1–10.

764 SAMHSA, 2019. Substance Abuse and Mental Health Services Administration. Key substance
765 use and mental health indicators in the United States: Results from the 2018 National
766 Survey on Drug Use and Health (HHS Publication No. PEP19-5068, NSDUH Series H-
767 54). Rockville, MD: Center for Behavioral Health Statistics and Quality, Substance Abuse
768 and Mental Health Services Administration. https://www.samhsa.gov/data/ (accessed
769 2020/11/10).
770 Schultz, M. M.; Furlong, E. T.; Kolpin, D. W.; Werner, S. L.; Schoernfuss, H. L.; Barber, L. B.;
771 Blazer, V. S.; Norris, D. O.; Vajda, A. M., 2010. Antidepressant pharmaceuticals in two
772 U.S. effluent-impacted streams: occurrence and fate in water and sediment, and selective
773 uptake in fish neural tissue. Environ, Sci. Technol. 44, 1918-1925.
774 SCORE (Sewage Analysis CORe Group Europe), 2019: SCORE monitoring 2019. Avaialble at
775 https://score-cost.eu/wp-
776 content/uploads/sites/118/2020/03/SCORE_2019_publish_12m.pdf. (accessed
777 2020/11/10).
778 Sharma, P., Gupta, S., Chaudhary, M., Mitra, S., Chawla, B., Khursheed, M. A., Ramachandran,
779 R., 2019. Oct4 mediates Müller glia reprogramming and cell cycle exit during retina
780 regeneration in zebrafish. Life Sci. Alliance. 2, e201900548.
781
782 Shin, D., Shin, J. Y., McManus, M. T., Ptácek, L. J., Fu, Y. H., 2009. Dicer ablation in
783 oligodendrocytes provokes neuronal impairment in mice. Ann Neurol. 66, 843-857.
784 Skariah, G., Seimetz, J., Norsworthy, M., Lannom, M. C., Kenny, P. J., Elrakhawy, M.,
785 Forsthoefel, C., Drnevich, J., Kalsotra, A., Ceman, S., 2017. Mov10 suppresses
786 retroelements and regulates neuronal development and function in the developing brain.
787 BMC Biol. 15, 54.
788 Skees, A. J, Foppe, K. S., Loganathan, B., Subedi, B., 2018. Contamination profiles, mass
789 loadings, and sewage epidemiology of neuropsychiatric and illicit drugs in wastewater and
790 river waters from a community in the Midwestern United States. Sci. Total. Environ. 631-
791 632, 1457-1464.
792 Sperlágh, B., Köfalvi, A., Deuchars, J., Atkinson, L., Milligan, C. J., Buckley, N. J., Vizi, E. S.,
793 2002. Involvement of P2X7 receptors in the regulation of neurotransmitter release in the
794 rat hippocampus. J. Neurochem. 81, 1196-1211.
795 Stelzer, G., Rosen, N., Plaschkes, I., Zimmerman, S., Twik, M., Fishilevich, S., Stein, T. I.,
796 Nudel, R., Lieder, I., Mazor, Y., Kaplan, S., Dahary, D., Warshawsky, D., Guan-Golan,
797 Y., Kohn, A., Rappaport, N., Safran, M., Lancet, D., 2016. The GeneCards Suite: From
798 Gene Data Mining to Disease Genome Sequence Analyses. Curr. Protoc. Bioinformatics.
799 54, 1.30.1–1.30.33.
800 Stewart, A.; Reihl, R.; Wong, K.; Green, J.; Cosgrove, J.; Vollmer, K.; Kuzer, E.; Hart, P.;
801 Allain, A.; Cachat, K.; Gaikwad, S.; Hook, M.; Rhymes, K.; Newman, A.; Utterback, E.;
802 Chang, K.; Kalueff, A.V., 2011. Behavioral effects of MDMA ("Ecstasy") on adult
803 zebrafish. Behav. Pharmacol. 22, 275-280.
804 Subedi, B.; Kannan, K., 2014. Mass loading and removal of select illicit drugs in two wastewater
805 treatment plants in New York State and estimation of illicit drug usage in communities
806 through wastewater analysis. Environ. Sci. Technol. 48, 6661-6670.

Subedi, B.; Kannan, K., 2015. Occurrence and fate of select psychoactive pharmaceuticals and antihypertensives in two wastewater treatment plants in New York State, USA. Sci. Total. Environ. 514, 273-280.
Takiyama Y., 2007. Sacsinopathies: sacsin-related ataxia. Cerebellum 6, 353–359.
Thisse, B., Thisse, C., 2004. Fast Release Clones: A High Throughput Expression Analysis. ZFIN Direct Data Submission.
Thompson, W. A.; Arnold, V. I.; Vijayan, M. M., 2017. Venlafaxine in embryos stimulates neurogenesis and disrupts larval behavior in Zebrafish. Environ. Sci. Technol. 51, 12889-12897.
Trapnell, C.; Roberts, A.; Goff, L.; Pertea, G.; Kim, D.; Kelley, D. R.; Pimentel, H.; Salzberg, S. L.; Rinn, J. L.; Pachter, L., 2012. Differential gene and transcript expression analysis of RNA-seq experiments with TopHat and Cufflinks. Nat. Protoc. 7, 562-578.
Ueda, H. R., Hayashi, S., Chen, W., Sano, M., Machida, M., Shigeyoshi, Y., Iino, M., Hashimoto, S., 2005. System-level identification of transcriptional circuits underlying mammalian circadian clocks. Nat. Genet. 37, 187-192.
Uhlén, M., Fagerberg, L., Hallström, B. M., Lindskog, C., Oksvold, P., Mardinoglu, A., Sivertsson, Å., Kampf, C., Sjöstedt, E., Asplund, A., Olsson, I., Edlund, K., Lundberg, E., Navani, S., Szigyarto, C. A., Odeberg, J., Djureinovic, D., Takanen, J. O., Hober, S., Alm, T., Edqvist, P. H., Berling, H., Tegel, H., Mulder, J., Rockberg, J., Nilsson, P., Schwenk, J. M., Hamsten, M., von Feilitzen, K., Forsberg, M., Persson, L., Johansson, F., Zwahlen, M., von Heijne, G., Nielsen, J., Pontén, F., 2015. Proteomics. Tissue-based map of the human proteome. Science 347, 1260419.
Watanabe, K.; Batikian, C. M.; Pelley, D.; Carlson, B.; Pitt, J.; Gersberg, R. M., 2020. Occurrence of stimulant drugs of abuse in a San Diego, CA, stream and their consumption rates in the neighboring community. Water Air Soil Pollut. 231, 202-213.
Wu, S., Xue, R., Hassan, S., Nguyen, T. M. L., Wang, T., Pan, H., Xu, J., Liu, Q., Zhang, W., Wen, Z., 2018. Il34-Csf1r pathway regulates the migration and colonization of microglial precursors. Dev. Cell 46, 552-563.
Yates, A. D.; Achuthan, P.; Akanni, W.; Allen, J.; Allen, J.; Alvarez-Jarreta, J., 2020. Ensembl 2020. Nucleic Acids Res. 8, D682-D688.
Yuan, Q., Zhang, S., Li, J., Xiao, J., Li, X., Yang, J., Lu, D., Wang, Y., 2020. Comprehensive analysis of core genes and key pathways in Parkinson's disease. Am. J. Transl. Res. 12, 5630-5639.
Zechel S., Huber-Wittmer, K., von Bohlen und Halbach O., 2006. Distribution of the iron-regulating protein hepcidin in the murine central nervous system. J. Neurosci. Res. 84, 790-800.

Table 1. Average rate of drug discharge through the wastewater effluent and average level of drug residues in the receiving creek. The values in parenthesis represent the detection frequency of drugs through seven consecutive days.

Analytes*	**Discharge Rate (mg/d/1000 people) ± 95% Confidence Interval		Concentration (ng/L) ± Standard Error		
	WWTP-A	WWTP-B	Creek-A	Creek-B	Literature
Stimulants					
Cocaine	9.01 ± 6.27	10.6 ± 17.7	11.5 ± 2.37 (100%)	14.9 ± 5.45 (100%)	5.26[a]; 8-53[e]; 2.50-3.40[f];
Benzoylecgonine	23.0 ± 12.6	23.8 ± 13.5	23.4 ± 3.67 (43%)	18.6 ± 0.76 (29%)	9.48[a]; 8-60[e]; 2.40-14.2[f];
Norcocaine	7.19 ± 2.37	2.97 ± 2.55	11.3 ± 0.80 (100%)	10.6 ± 0.89 (100%)	3.70-4.40[f];
Cocaethylene	nd	nd	2.05 (14%)	2.55 ± 0.44 (43%)	
Methamphetamine	18.1 ± 7.49	11.8 ± 10.5	18.4 ± 5.35 (57%)	15.2 ± 2.36 (29%)	1.3-62.6[b]; 7[c]; 24-1994[e]; 2.70-86.4[f];
Amphetamine	3.44 ± 1.44	3.91 ± 1.84	3.06 ± 1.31 (29%)	2.32 ± 0.20 (29%)	3-630[c]; 9-101[e]; 2.50-5.10[f];
Methylphenidate	3.59 ± 1.15	3.10 ± 1.23	2.92 (14%)	3.41 (14%)	2.70-3.90[f];
Opioids/Narcotics					
Heroin	1263 ± 1180	692 ± 1050	262 ± 84.3 (100%)	434 ± 143 (86%)	
6-acetyl Morphine	2.18	1.86	nd	nd	
Morphine	5.05 ± 3.22	10.3 ± 74.0	10.7 ± 3.79 (43%)	14.1 ± 4. 95 (43%)	16-83[c]; 6.2[f];
Methadone	17.2 ± 3.74	9.67 ± 5.07	19.2 ± 1.83 (100%)	8.31 ± 2.03 (100%)	2.4-17.8[f];
EDDP	59.4 ± 13.8	44.6 ± 20.6	71.7 ± 5.27 (100%)	42.3 ± 3.80 (100%)	
Codeine	12.7 ± 2.97	10.5 ± 5.64	13.1 ± 2.27 (100%)	15.1 ± 2.99 (57%)	4.20-34.4[f];
Fentanyl	3.60 ± 1.63	2.47	4.93 ± 0.87 (71%)	3.90 ± 0.92 (29%)	1.40-1.50[f];
Oxycodone	43.3 ± 9.01	22.8 ± 11.8	51.1 ± 4.41 (100%)	24.9 ± 6.31 (100%)	2.90-27.0[f];
Hydrocodone	21.4 ± 3.65	9.59 ± 5.06	21.9 ± 3.73 (100%)	11.2 ± 0.97 (43%)	5.00-126[f];
Hydromorphone	1.77 ± 1.20	3.22	4.67 ± 1.00 (57%)	3.34 ± 0.15 (43%)	9.10[f];
Buprenorphine	nd	3.40	5.88 (14%)	nd	
Hallucinogens					
MDMA	nd	nd	nd	nd	6.1[f];
MDEA	nd	nd	nd	nd	
MDA	11.5 ± 4.12	8.95 ± 4.80	8.22 ± 0.76 (100%)	8.86 ± 0.77 (100%)	
THC	nd	nd	nd	nd	
THC-OH	nd	nd	nd	nd	51.6-339[f];
THC-COOH	nd	nd	nd	nd	
Antischizophrenics					
Quetiapine	nd	nd	4.18 (14%)	nd	4.4[f];
Aripiprazole	3.52	nd	0.91 ± 0.30 (86%)	0.79 ± 0.14 (100%)	5.1-8.3[f];
Anxiolytics					
Lorazepam	6.25 ± 0.87	6.71 ± 2.79	4.99 ± 0.88 (100%)	6.06 ± 0.87 (57%)	15.8[f];
Alprazolam	2.44 ± 1.45	575 ± 117	3.29 (14%)	nd	0.37[a]; 2.40-6.10[f];
Diazepam	3.51 ± 4.54	1.15 ± 8.42	3.25 ± 0.01 (29%)	3.16 ± 0.22 (57%)	2.60-6.10[f];
Oxazepam	5.34 ± 1.28	4.36 ± 3.72	8.97 ± 1.35 (100%)	5.66 ± 1.38 (100%)	22.5-34.5[f];
Temazepam	19.6 ± 5.90	30.1 ± 13.0	46.7 ± 6.51 (100%)	41.9 ± 5.83 (100%)	3.40-60.9[f];
Carbamazepine	92.6 ± 20.0	89.7 ± 43.7	168 ± 13.9 (100%)	129 ± 14.3 (100%)	36.7[a]; 3.1-296[b];6-38[c]; 3.80-63.1[f];
Antidepressants					

Sertraline	34.8 ± 11.6	25.7 ± 13.9	53.9 ± 6.20 (100%)	29.9 ± 4.50 (100%)	0.7-37.5[d]; 3.80.-24.2[f];
Fluoxetine	19.5 ± 5.98	25.9 ± 11.8	26.8 ± 1.75 (100%)	25.8 ± 1.87 (100%)	4.52[a]; 0.5-43.2[d]; 3.50-9.60[f];
Venlafaxine	222 ± 44.3	155 ± 89.7	364± 36.8 (100%)	212± 62.05 (100%)	73.3-690[d]; 2.60-243[f];
Citalopram	116 ± 22.2	55.4 ± 43.9	170± 20.3 (100%)	78.7 ± 29.34 (100%)	4.53-219[d]; 2.70-3.90[f];

*metabolites are italicized; nd: not detected

**estimated population of community A and B were 189,335 and 157,796, respectively, based on quantified ammoniacal nitrogen load to the WWTPs (Croft et al., 2020)

[a]Fifty Minnesota Lakes in Minnesota (Ferrey et al., 2015)

[b]Wastewater impacted surface water in Omaha, NE (Bartelt-Hunt et al., 2009)

[c]Gwynns Falls and Oregon Ridge watershed in Baltimore, MD (Lee et al., 2016)

[d]Boulder Creek, CO and Fourmile Creek, IA (Schultz et al., 2010)

[e]Forester Creek, Santee, CA (Watanabe et al., 2020)

[f]Bee Creek and Clarks River, Murray, KY (Skees et al., 2018)

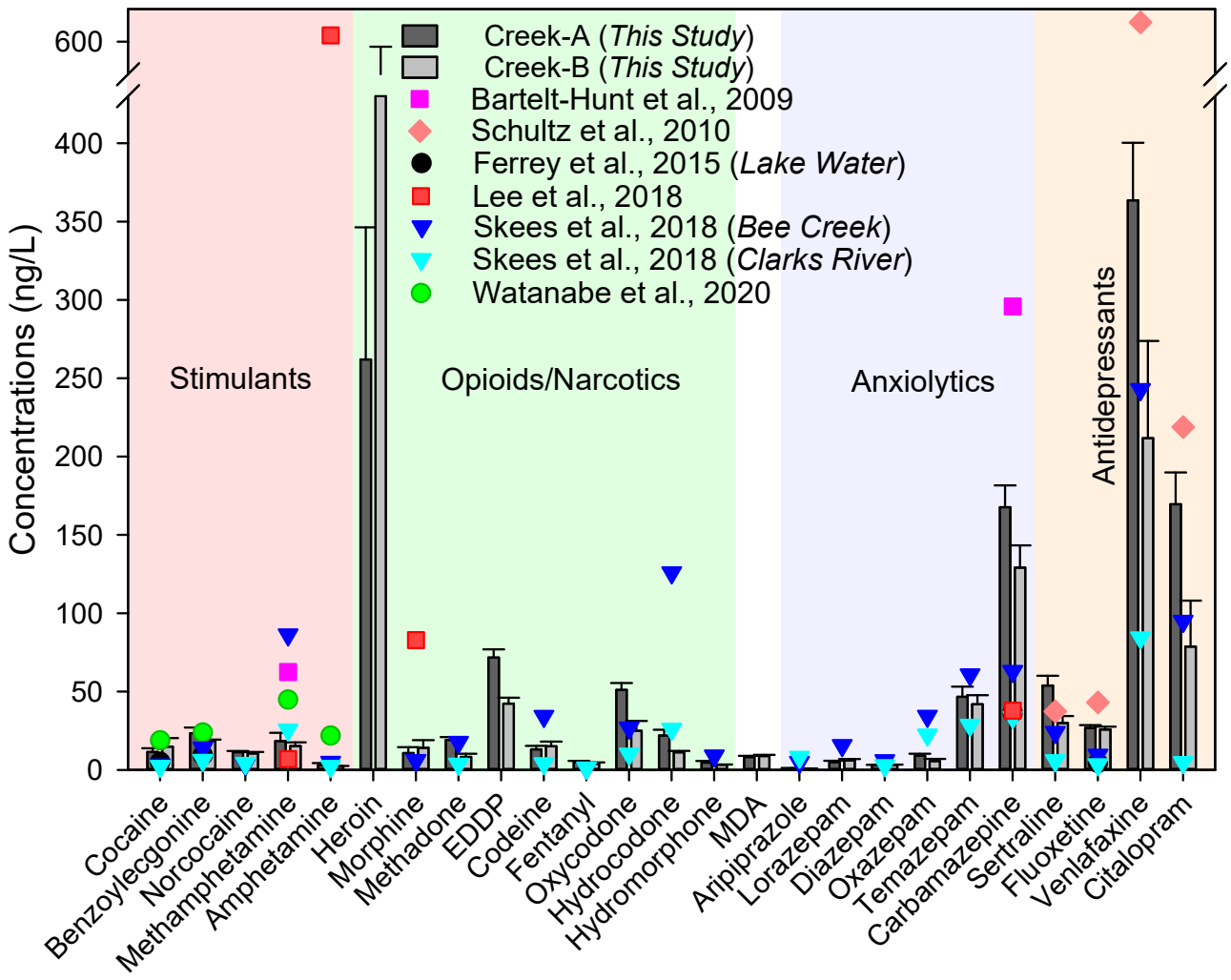

857

858 **Figure 1**. Concentration of illicit and prescribed antipsychotic drug residues in two treated wastewater receiving creeks in Eastern

859 Kentucky (this study) and surface water elsewhere in the U.S.

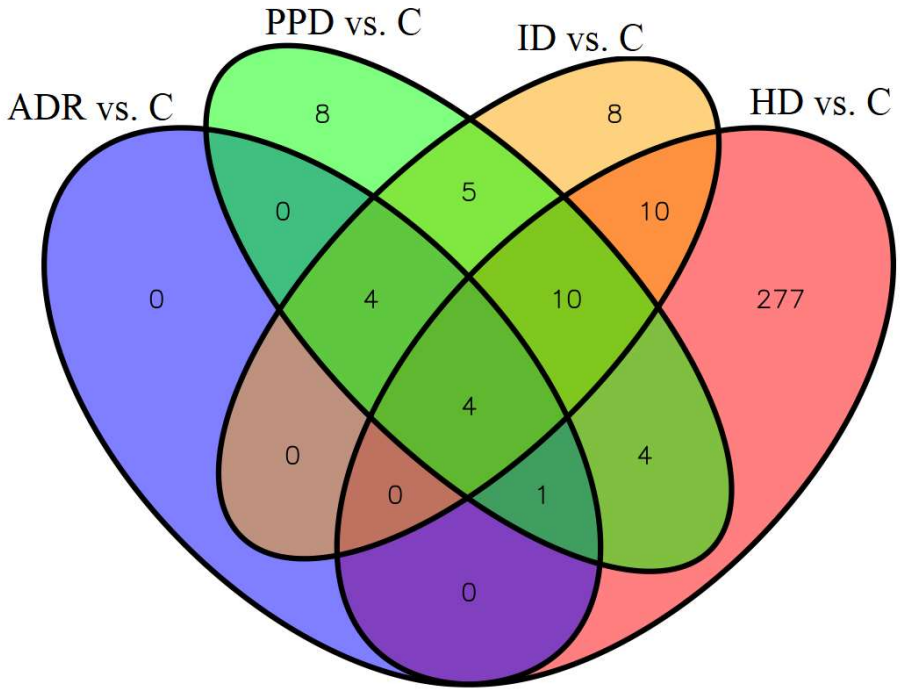

860

861 **Figure 2.** The number of common and unique differentially expressed genes across comparisons. The differentially expressed genes
862 were mostly unique to the high dose mixture groups, though some genes were also differentially expressed in the other groups with
863 varying degrees of overlap. ADR: mixture of all drug residues quantified in creeks A and B; PPD: mixture of all prescribed psychotic
864 drug residues quantified in creeks A and B; ID: mixture of all illicit drug residues quantified in creeks A and B; HD: high dose mixture
865 of all target drug residues reported in surface water elsewhere at the highest concentrations; C: control.

866

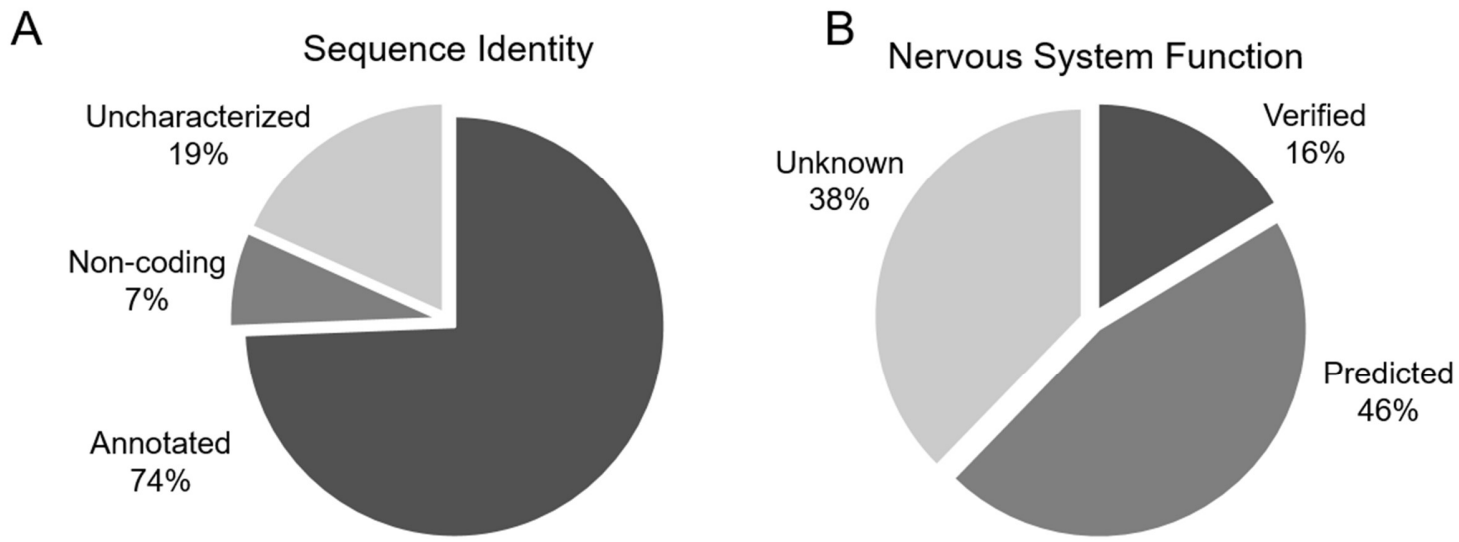

867

868 **Figure 3.** Of the top differentially expressed sequences, approximately 25% represent novel or non-protein-coding genes (A). Of the

869 annotated differentially expressed sequences, most have verified or predicted nervous system function (B).

870

871